J Neurophysiol 125: 2144–2157, 2021.
First published May 5, 2021; doi:10.1152/jn.00559.2020

american physiological society

JNP JOURNAL OF NEUROPHYSIOLOGY

RESEARCH ARTICLE

Higher Neural Functions and Behavior

The roles of the lateral intraparietal area and frontal eye field in guiding eye movements in free viewing search behavior

Koorosh Mirpour[1] and James W. Bisley[1,2,3]

[1]*Department of Neurobiology, David Geffen School of Medicine at UCLA, Los Angeles, California;* [2]*Jules Stein Eye Institute, David Geffen School of Medicine at UCLA, Los Angeles, California; and* [3]*Department of Psychology and the Brain Research Institute, UCLA, Los Angeles, California*

Abstract

The lateral intraparietal area (LIP) and frontal eye field (FEF) have been shown to play significant roles in oculomotor control, yet most studies have found that the two areas behave similarly. To identify the unique roles each area plays in guiding eye movements, we recorded 200 LIP neurons and 231 FEF neurons from four animals performing a free viewing visual foraging task. We analyzed how neuronal responses were modulated by stimulus identity and the animals' choice of where to make a saccade. We additionally analyzed the comodulation of the sensory signals and the choice signal to identify how the sensory signals drove the choice. We found a clearly defined division of labor: LIP provided a stable map integrating task rules and stimulus identity, whereas FEF responses were dynamic, representing more complex information and, just before the saccade, were integrated with task rules and stimulus identity to decide where to move the eye.

NEW & NOTEWORTHY The lateral intrapareital area (LIP) and frontal eye field (FEF) are known to contribute to guiding eye movements, but little is known about the unique roles that each area plays. Using a free viewing visual search task, we found that LIP provides a stable map of the visual world, integrating task rules and stimulus identity. FEF activity is consistently modulated by more complex information but, just before the saccade, integrates all the information to make the final decision about where to move.

eye movement; frontal eye field; lateral intraparietal; visual search

INTRODUCTION

We make thousands of small sensory-motor decisions every day, particularly in the oculomotor system, which guides 2 to 3 eye movements/s. A long line of electrophysiology studies have established that the frontal eye field (FEF) of prefrontal cortex and the lateral intraparietal area (LIP) of posterior parietal cortex play a role in guiding covert attention (1–4) and eye movements (5–8). Physiologically, neurons in both areas behave quite similarly. They respond to inherently salient stimuli (9, 10), have responses that are modified by top-down, endogenous factors (11–14) and display persistent activity in the memory-guided saccade task (6, 15). However, some differences remain. Low current microstimulation of FEF generates saccades (16), whereas in LIP much higher currents are needed (17) and the results are not always consistent (18, 19). And a subset of FEF neurons respond to learned saccades made in the dark (6), whereas LIP neurons do not.

Insights from the physiological and psychological literature have provided a computational framework for the guidance of attention and eye movements: the saliency map model (20), which we refer to as a priority map to highlight the fact that it is not primarily driven by visual salience (21). This model integrates bottom-up sensory and top-down cognitive information and neuronal correlates of these responses have been shown in both LIP and FEF (22, 23). Yet it is not clear what unique roles LIP and FEF play in this framework. Several studies have suggested that salience or bottom up sensory processing originates in LIP, whereas the top-down control of attention (11, 24) and eye movements (25) are driven by FEF. These conclusions, however, were based on when differences emerged in population responses within these areas and while they showed some differences

Correspondence: K. Mirpour (mirpour@gmail.com).
Submitted 18 September 2020 / Revised 17 March 2021 / Accepted 28 April 2021

in the overall timing and magnitude of the top-down and bottom up signals, they did not identify differences in mechanistic processing within each of the areas.

One of the reasons that differences between LIP and FEF have not been clearly identified might be the general use of oversimplified behavioral tasks. For example, a single saccade decision task or center-out visual search tasks lack the strategic planning and influence of clutter that affect behavior in natural visual search. The absence of such factors could simplify and decrease the diversity of neuronal responses recorded in these tasks. In this study, we take advantage of a free viewing visual search task that mimics the natural dynamics and interactions of natural viewing to computationally identify the specific roles of LIP and FEF.

Previous studies have explored the oculomotor responses of FEF neurons during free viewing of natural stimuli (26–28). We have combined these findings with previous work from our laboratory (22, 29–31) to hypothesize distinct roles of LIP and FEF in naturalistic viewing behavior (32). Specifically, we hypothesized that LIP neurons represent a robust time invariant priority map, integrating sensory and cognitive signals, whereas the FEF representation is more dynamic and controls the flow of saccadic behavior.

To test this hypothesis, we examined how sensory information and the resultant decision about where to look modulated and, combined, comodulated activity in populations of LIP and FEF neurons during maintained fixation within ongoing search. We found that LIP and FEF work as a collaborative network, each playing a role in guiding the timing and location of upcoming saccades: within a fixation, LIP activity was consistently modulated by both the identity of the stimulus in the RF and whether a saccade would be made to that stimulus, whereas activity in FEF was only comodulated by these factors immediately before the saccade, although other factors that affected the saccade choice were represented throughout the fixation.

METHODS

All experiments were approved by the Chancellor's Animal Research Committee at UCLA as complying with the guidelines established in the Public Health Service Guide for the Care and Use of Laboratory Animals. Neuronal and behavioral data were collected from four male rhesus macaques (8–12 kg). The animals were implanted with head posts, scleral coils, and recording cylinders during sterile surgery under general anesthesia (22); animals were initially anesthetized with ketamine and xylazine and maintained with isofluorane. Surgery was conducted using aseptic techniques and analgesics and antibiotics were provided during postoperative recovery. The data sets of this paper were analyzed in previous studies (22, 29–31, 33–35), although all the analyses presented in the current paper are novel and have not been published before.

Behavioral Tasks

The behavioral paradigms were controlled using REX system (36) and stimuli were presented with the associated VEX system from the Laboratory of Sensorimotor Research at the National Eye Institute. All animals were trained on a standard memory-guided saccade task and the visual foraging task (22).

The memory guided saccade task was used for mapping the receptive field (RF) of each recorded neuron and for physiological confirmation that neurons were recorded from LIP and FEF. In the memory guided saccade task, animals started a trial by fixating on a white fixation point on the center of the screen. After 300 ms to 500 ms of fixating, a peripheral target flashed for 200 ms. Animals were to memorize the location of the target and, after a 600-ms delay, make an eye movement to it within 450 ms after disappearance of the fixation point.

Animals started the foraging task by fixating on a fixation point appearing on the center, left or right of the screen. After 450 to 700 ms of stable fixation, an array of 10 objects consisting 5 potential targets (T) and 5 distractors (+) appeared on the screen (Fig. 1*A*). In each recording session, visual stimuli were arranged in a way that when animals were gazing at one of the stimuli (small circle in Fig. 1*A*) one other stimulus could fall into the receptive field of the recorded neuron (big oval in Fig. 1*A*). Note that for some LIP neurons, the number of Ts and distractors varied from trial to trial (29), but only data from trials with 5 Ts and 5 distractors are included in the current analyses. On each trial, one of the Ts was loaded with a drop of juice as a reward. To get the reward, the animals had to fixate the target for 500 ms within 8 s of array onset. For the analyses described here, we define a target as an unfixated T (i.e., a T that has not been fixated earlier in the trial). For detailed analyses of the behavioral task from two of the animals see Mirpour et al. (22).

Electrophysiological Recording

We recorded extracellular single-unit activity from 200 LIP neurons (26 from monkey C, 81 from monkey D, and 93 from monkey E) and 231 FEF neurons (78 from monkey E and 153 from monkey M) using microelectrodes inserted through a guide tube into the cortex. Neurons were not recorded simultaneously in the two areas. Activity was recorded using the Plexon Multichannel Acquisition Processor (MAP) and spikes were sorted using the SortClient software (Plexon Inc., Dallas, TX) or was recorded using the MEX pattern spike sorter and recorded in real time [54 LIP neurons from Mirpour et al. (22)]. Anatomical locations of the recordings were defined by MRI and confirmed by the pattern of responses to the memory guided saccade task. Recorded neurons were considered to be in LIP if they showed the typical pattern of LIP activity consisting of a visual burst, delayed sustained activity and/or a peri-saccadic burst, during the memory-guided saccade task (5). We confirmed the FEF locations by evoking saccades using low current microstimulation (70 ms train of biphasic pulses, negative first, 0.2 ms width/pulse phase, delivered at a frequency of 330 Hz) while animals performed a blink task (37). Neurons were recorded if they showed increased activity during the visual, memory, or movement stage of the memory-guided saccade. Consequently, fixation neurons (38, 39) were excluded from this study.

The size and position of the receptive field of each neuron was mapped using an automated memory guided saccade task, covering 9 (in a confined 3 × 3 grid) and then 25 (in a confined 5 × 5 grid) locations (40). Figure 2 shows the means ± SE

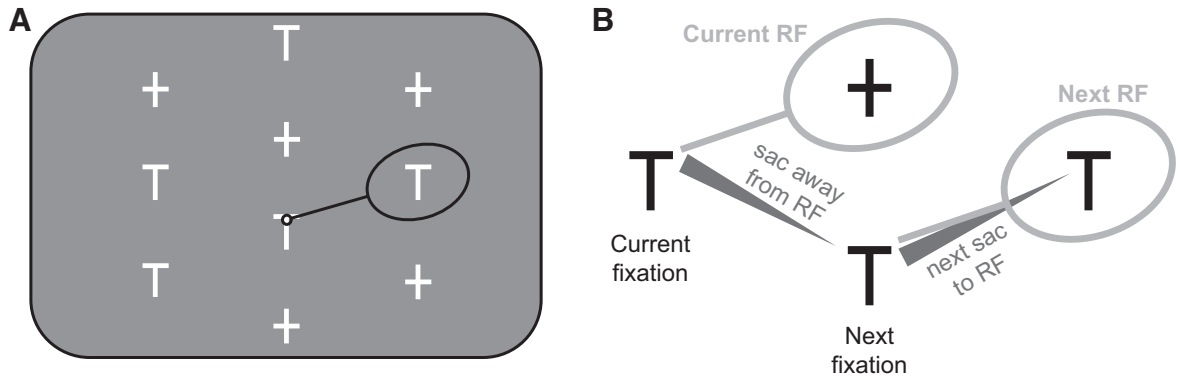

Figure 1. Behavioral paradigm. *A*: in each trial, 5 potential targets (T shaped) and 5 distractors (+ shaped) were presented after the animal had fixated the fixation point for at least 450 ms. One of the potential targets was loaded with a reward, which the animal received if it fixated that target for 500 ms. The stimuli were arranged in a way that when the animals looked at one object (small circle), a single other object was usually inside the receptive field (RF) of recorded neuron (oval). *B*: a schematic diagram of a series of eye movements from left to right during the visual foraging task. For each fixation, there was an object at the fovea and an object inside receptive field.

normalized population responses of 218 FEF neurons in the memory-guided saccade task. These data pool all locations found to be within each neurons' receptive field and, thus, are not as clean as when a single target location is used. However, they show that the population of neurons we recorded from included visual, delay, and movement-related responses. Neurons were excluded from the study if their receptive fields were so large that they would encompass two or more stimuli in the array when fixating another stimulus. All the neural data analyzed here were collected from the foraging task, which was run after mapping the receptive field using memory-guided saccades.

Data Analysis

Data analyses were performed using custom code written in MATLAB (MathWorks Inc.). Each trial from the visual foraging task was separated to fixations. The first fixation of the trial always started at the fixation point and for 51 LIP and 158 FEF neurons, the point changed to one of the objects when the array appeared. For the remaining neurons, the fixation point was outside of the array and was not replaced by a stimulus. Most of the analyses were done on fixations that occurred after the first saccade, which we refer to as "ongoing search." For these data, the neural responses were aligned by the start of fixation (i.e., the end of the previous saccade) or the start of the next saccade (i.e., the end of the fixation). The onset of saccades were detected by using an eye-velocity detection algorithm. Fixation durations were typically bimodal, with modes around 180–200 ms and 600–700 ms and a trough around 300–350 ms depending on the animal [see Fig. 2 in Mirpour et al. (22) and Fig. 2 in Mirpour et al. (30)]. Except where noted, analyses were done on fixations lasing a minimum of 300 ms. Similar, albeit much noisier, results were seen for fixations lasting between 150 ms and 300 ms.

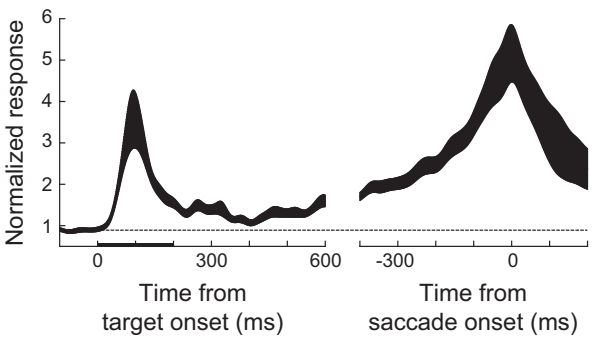

Figure 2. Mean ± SE normalized population responses of 218 FEF neurons in the memory-guided saccade task, aligned by target onset (*left*) and saccade onset (*right*). The target was presented for 200 ms and the delay period between target offset and the go signal was 600 ms. The solid black line on the *x*-axis represents the time the target was presented. The dashed line indicates baseline, as measured in the 100 ms before target onset. FEF, frontal eye field.

For visualization, the neural responses were presented as spike density functions (41) using a sigma of 10 ms, and were normalized by dividing the activity by a normalizing factor. The normalizing factor for each neuron was calculated as the average response over a 150 ms period starting 150 ms after fixation onset across all fixations that occurred after the first saccade, that lasted at least 300 ms and that had a target at the fovea and a distractor in the RF.

Within the foraging task, many factors change as the animals make eye movements from one object to another. In each fixation there could be an object in the RF and there was usually an object at the fovea. Although it is well known that many neurons in LIP and FEF are driven by the identity of the stimulus in the RF, we have recently shown that the response of FEF neurons is affected by fixation duration (31). Because animals typically fixate distractors for shorter durations than targets, we included the identity of the stimulus at the fovea as a factor to see whether this identity was a factor when using only long fixation durations (i.e., greater than 300 ms). The animal's behavior can also be characterized by whether the next saccade was made to the RF or away from it. Based on these conditions, we defined three main parameters: *1*) Choice: whether the animal made a saccade to or away from RF; *2*) RF objects: whether there was a target or distractor in RF; *3*) Foveal objects: whether there was a target or a distractor at fovea. These three parameters can be extracted about the current fixation or next fixation (Fig. 1*B*).

Therefore, six main parameters were calculated for every single fixation excluding the first fixation of each trial. For most conditions, we had a median of at least 200 fixations across neurons. The median number of fixations, median absolute deviation and quartiles of the number of fixations per condition are given in Table 1 ~20% of fixations resulted in a saccade into the RF.

For most of the analyses we were interested in looking at the information carried about the parameters instead of calculating the mean neural response to each stimulus. To measure this, we calculated the response modulation index (RMI). The RMI is a nonparametric measure based on neural response variability introduced by (42, 43). It quantifies the amount of information obtained about behavioral parameters in the neural data and closely resembles information-theoretic measures. We chose to use RMI over other information-theoretic measures because the number of repetitions per stimulus in our conditions were not equal and, in some cases, were too small for such analyses, which could potentially create biases. For each of the six parameters, we calculated the ratio of stimulus-to-stimulus variance across trials to average trial-to-trial variance using formula similar to the *f* test:

$$f_{\text{ratio}} \frac{\text{Var}_{\text{between}}}{\text{Var}_{\text{within}}},$$

where $\text{Var}_{\text{between}}$ is the stimulus-to-stimulus variance and $\text{Var}_{\text{within}}$ is the average trial-to-trial variance. This ratio is the equivalent to a signal-to-noise ratio. To normalize the value across all parameters, the stimulus identities for each fixation were shuffled and the ratio calculated again. The RMI is the original ratio divided by the average of 10^4 shuffles:

$$\text{RMI} = \frac{\text{data } f_{\text{ratio}}}{\text{randomized } f_{\text{ratio}}},$$

This normalization of the f_{ratio} by the randomized f_{ratio} corrects for deviations of the data set from normality and any inherent variance of neural data due to other task-irrelevant factors. For each neuron, the RMI for each parameter was calculated from 400 ms before start of fixation to 400 after it using 50 ms windows with 5 ms steps. We also ran this analysis using bins with equal numbers of spikes, as the use of equal bin width could bias modulation during bins of low average responses. The results for both analyses were qualitatively very similar, so here we show only the analysis in which the time bins were kept constant. To simplify the results and exclude possible interactions or collinearity among factors, we only calculated the main effects (i.e., explained variance of one main factor). Interactions (i.e., the explained variance of nonlinear combinations of the factors) were ignored.

Table 1. *The median, median absolute deviation, and quartiles of the number of fixations per neuron for each condition for fixations lasting at least 300 ms and occurring after the first saccade*

Condition	Median	MAD	First Quartile	Third Quartile
LIP				
Distractor at fovea	379.6	512.1	5	1,971
Target at fovea	481.3	433.6	18	1,879
Distractor in RF	212.9	225.0	9	1,090
Target in RF	196.0	213.4	5	1,195
FEF				
Distractor at fovea	33.4	51.3	4	3,32
Target at fovea	955.6	441.5	92	2,509
Distractor in RF	352.3	195.4	16	1,194
Target in RF	297.2	165.2	23	1,025

Note that saccades to the RF occurred in approximately 20% of fixations. FEF, frontal eye field; LIP, lateral intraparietal area; MAD, median absolute deviation; RF, receptive field.

To calculate the chance level RMI for each neuron, we calculated the average RMI with shuffled stimulus tags, keeping the number of trials in each category unchanged for 10^3 iterations. To calculate whether the RMI for a given time bin was significant across the population, the RMI values were compared with averaged shuffled RMI across neurons using paired one-tailed (because RMI values should only be greater than the shuffled data) Wilcoxon signed rank tests with an α of 0.005 indicating significance.

A key question we are interested in is how information about stimulus identity drives the behavior across the neural population. To answer this, we calculated a metric to represent the integration of the animal's saccadic choice and stimulus identity. Specifically, we calculated the comodulation of the choice RMI (saccade to or away from RF) and either the RF object RMI (target or distractor in RF) or the fovea object RMI (target or distractor in fovea) using the formula:

$$\text{Comodulation} = \frac{1}{n} \sum_1^n (X - \overline{X})(Y - \overline{Y}),$$

where n is the number of neurons, X and Y are the single cell RMIs for the two variables (for example choice and RF object) and $\overline{X}$ and $\overline{Y}$ are the average RMIs for the two variables. The calculation and value of the comodulation is very similar to a correlation coefficient: the reliability depends on the magnitude of the value and on the number of observations. Thus, to test if the comodulation values of bins are significantly different from zero, we used a linear regression *t* test which is a commonly used for testing Pearson correlation coefficients. First the comodulation values of all bins were normalized to maximum values during the time course of fixations. Then the *t* statistic was calculated using formula:

$$t = \frac{c\sqrt{n-2}}{\sqrt{1-c^2}},$$

where c is the comodulation value, n is the number of neurons contributing to each epoch, and t is the t statistic. The right tailed P value of each bin was calculated for t statistics using t distribution with an α of 0.005 indicating significance.

For the purpose of illustrating the individual neuron RMI traces in Fig. 6, outlier RMI traces were removed. Outliers were traces more than 4 scaled median absolute deviation (MAD) from the median. The scaled MAD is defined as:

$$\text{MAD} = c \times \text{median}(|x - \text{median}(x)|),$$

where x is the RMI values of the population, $c = 1.4826$, a constant linked to the assumption of normality of the data, disregarding the abnormality induced by outliers (44). The number of traces removed are listed in the figure legend. Critically, these outliers were included in the main population analyses.

RESULTS

To compare the dynamics of neuronal activity in LIP and FEF in naturalistic behavior, we trained four monkeys to forage for a reward loaded target by freely moving their eyes among 10 objects (Fig. 1*A*). The animals had to fixate the target for 500 ms to get the reward. No eye movements or fixations were punished: the trial ended either when the animal obtained the reward or after 8 s of search. We recorded the activity from single neurons using extracellular electrodes while the animals performed the task. The stimulus array was set up so that when the animal fixated one stimulus (small circle, Fig. 1*A*), no more than one other stimulus was in the RF (large oval, Fig. 1*A*). We analyzed the data from fixations lasting at least 300 ms as a function of the identity of the stimulus in the RF, the identity of the stimulus at the fovea and by the direction of the upcoming saccade (to or away from the RF), which we refer to as representing the animal's choice.

Neuronal Responses in LIP and FEF

At the start of each trial, the animals fixated a fixation point, after which the array of stimuli appeared on the screen. In a subset of sessions, in which 110 LIP and 179 FEF neurons were recorded, a stimulus appeared in the neuron's RF when the array appeared. The appearance of a stimulus in the RF increased the average response of neurons in both FEF and LIP (Fig. 3, *A* and *B*). These figures show responses from fixations lasting at least 350 ms and in which a saccade was made away from the RF. The response peaked around the same time in both areas after stimulus presentation. When looking in a 300-ms window starting 50 ms after array onset, the average population response in both areas responded significantly more to targets than distractors (Fig. 4, *A* and *B*). Although a subset of neurons in each area individually responded significantly more to a target appearing in the RF than to a distractor ($P < 0.05$, *t* test), the strength of this effect was greater in LIP, as seen by the greater deviations below the unity line in Fig. 4*A* compared with Fig. 4*B*, as was the proportion of neurons with individual differences: 30/110 (27.3%) in LIP and 18/179 (10.0%) in FEF ($\chi^2 = 14.58$, $P = 1.34 \times 10^{-4}$, χ^2 test). Although both areas showed a significant difference in response, the onset of the difference in response happened ~40 ms earlier in the FEF population (140 ms after array onset in FEF and 184 ms after array onset in LIP neurons). This was calculated as the first of 50 significant bins in a row at $P < 0.05$ with a running Wilcoxon signed-ranked test on the smoothed traces in Fig. 3, *A* and *B*.

Despite these general similarities in responses in LIP and FEF, we also found a number of noticeable differences. The first is obvious when comparing Fig. 3, *C* and *D*: during ongoing search, LIP neuronal activity clearly differentiated between targets and distractors in the RF (Fig. 3*C*), whereas FEF did not (Fig. 3*D*). Using a 300-ms window starting 50 ms after fixation onset, the LIP population responded more to targets than distractors in ongoing search (Fig. 4*C*), with 16/124 (12.9%) single neurons showing this significantly ($P < 0.05$, *t* test). This classic priority map-like pattern of activity was not seen in the average population of FEF neurons (Fig. 3*D* and Fig. 4*D*), despite the difference being present in the same population when the array first appeared (Fig. 3*B*). Furthermore, we found little evidence that single FEF neurons showed this at levels beyond those expected by chance: only 18/231 (7.79%) neurons responded significantly more to a target than to a distractor, which is not significantly more than the expected 5% ($\chi^2 = 3.792$, $P = 0.0515$, χ^2 goodness-of-

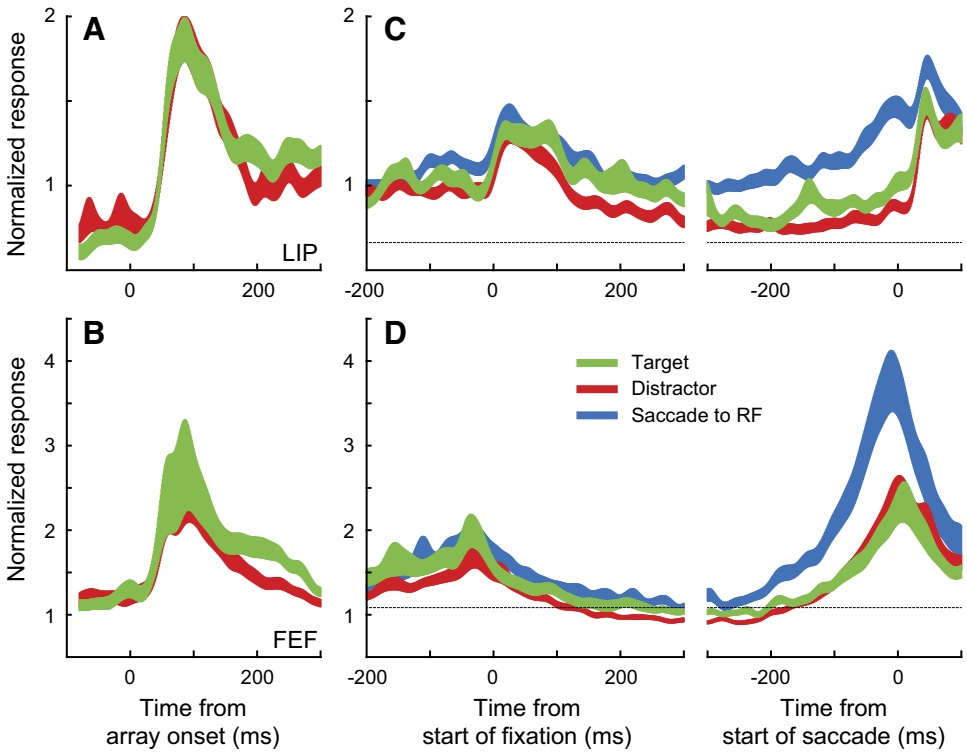

Figure 3. Mean ± SE normalized population responses of LIP and FEF neurons to targets (green traces) and distractors (red traces) in fixations lasting at least 350 ms and in which the saccade was made away from the receptive field or to targets in fixations lasting at least 350 ms in which the saccade was made into the receptive field (blue traces). The population response of 110 LIP neurons (*A*) and 179 FEF neurons (*B*) to array onset, aligned by array onset. The population response of 200 LIP neurons (*C*) and 231 FEF neurons (*D*) during ongoing visual search, aligned by the start of fixation (*left*) and the start of the next saccade (*right*). The dashed lines indicate baseline, as measured in a 100-ms window before array onset for all trials. Note that because *A* and *B* have only a subset of the neurons, the baseline in *C* and *D* does not perfectly match the prearray activity shown in *A* and *B*. FEF, frontal eye field; LIP, lateral intraparietal area; RF, receptive field.

fit test) and even fewer responded more to a distractor than to a target (13/231, 5.63%).

A second difference in the population responses is less obvious in this figure, but likely explains the first difference: the responses of FEF neurons are almost silenced during maintained fixation (31), whereas LIP neurons are not. A hint of this can be seen when comparing the response profiles in Fig. 3*B*, in which the FEF responses following the visual burst rapidly decline, to the response profiles in Fig. 3*A*, in which the LIP responses retain a moderate level of activity. During ongoing search (Fig. 3, *C* and *D*), responses in both areas appear to drop during maintained fixation, but mean LIP responses tend to remain above baseline levels (dashed line in Fig. 4*C*), whereas in most cases, FEF response dropped to or below baseline level (dashed line in Fig. 4*D*). To illustrate how these response profiles are different, we ran two analyses. We first tested whether LIP, like FEF, shows reduced activity during maintained fixation by comparing the responses in a 100-ms window, starting 50 ms after fixation on trials with long (≥350 ms) and short (>150 and <350) fixation durations. We found that the populations of neurons in both LIP (Fig. 4*E*) and FEF (Fig. 4*F*) responded more during shorter fixations than during longer fixations. However, a substantially higher proportion of FEF neurons (118/229) than LIP neurons (44/128) showed this difference significantly (χ^2 = 9.75, P = 0.0018). We then tested to see how strong this reduction of response was in each area, by comparing the activity in a 100-ms window starting 50 ms after fixation onset during long (≥350 ms) fixation durations, to the baseline response taken from a 200-ms window starting 200 ms before array onset. We found that a clear majority (137/200; Fig. 4*G*) of LIP neurons responded significantly more during maintained fixation than during baseline,

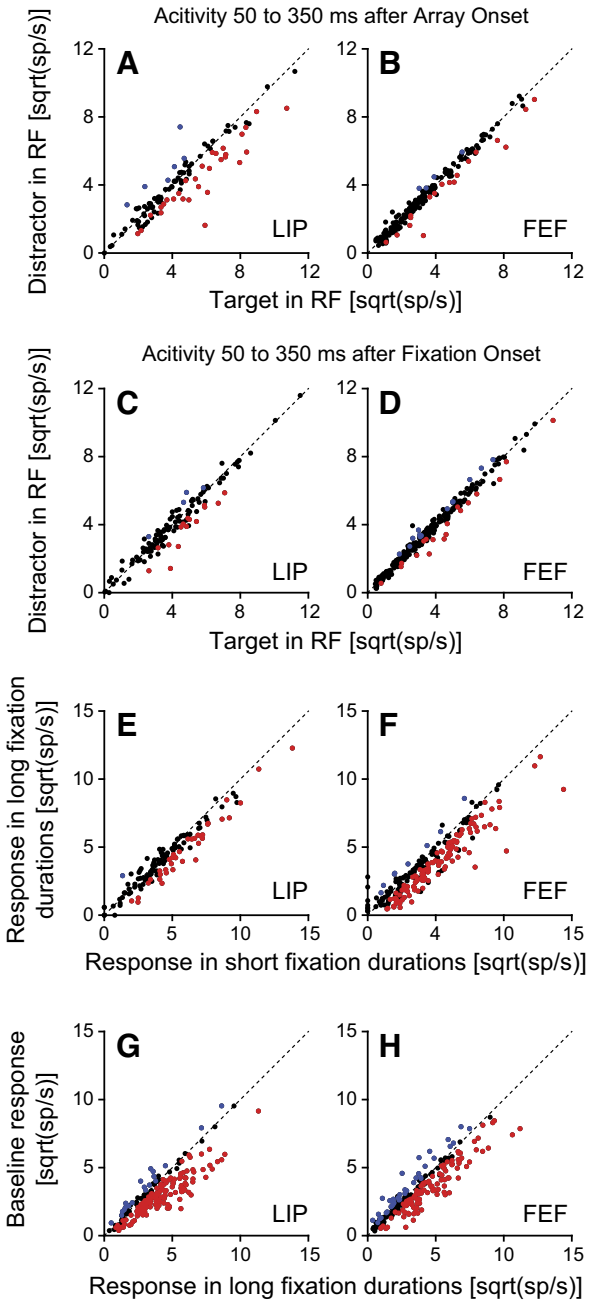

Figure 4. The responses of single neurons in the foraging task during fixations in which the next saccade would be made away from the receptive field (RF). *A*: the responses of 110 LIP neurons, following array onset. Thirty neurons (27.3%, red circles) had a significantly higher response to the targets and six neurons (5.5%, blue circles) had a significantly higher response to the distractors (two-tailed t test $P < 0.05$). The mean response was significantly stronger to a target than to a distractor (two-tailed Wilcoxon signed rank tests, n = 110, P = 0.00042, z = 3.52). *B*: the responses of 179 FEF neurons following array onset. Eighteen neurons (10.1%, red circles) had a significantly higher response to the targets and four neurons (2.2%, blue circles) had a significantly higher response to the distractors. The mean response was significantly stronger to a target than to a distractor (two-tailed Wilcoxon signed rank tests, n = 179, z = 2.33, P = 0.01969). *C*: the responses of 124 LIP neurons during ongoing search. Sixteen neurons (12.9%, red circles) had a significantly higher response to the targets and five neurons (4.3%, blue circles) had a significantly higher response to the distractors. The mean response was significantly stronger to a target than to a distractor (two-tailed Wilcoxon signed rank tests, n = 124, z = 2.8, P = 0.005086). *D*: the responses of 231 FEF neurons during ongoing search. Eighteen neurons (7.8%, red circles) had a significantly higher response to the targets and 13 neurons (5.6%, blue circles) had a significantly higher response to the distractor. There was no significant difference in the mean response to targets and distractors (two-tailed Wilcoxon signed rank tests, n = 231, z = 0.13, P = 0.8936). *E*: the responses of 128 LIP neurons in long and short fixation durations. Forty-four neurons (34.4%, red circles) had a significantly higher response during short fixations and only 1 (0.7%, blue circle) had a significantly higher response during long fixations ($P < 0.05$; two-tailed t tests). The mean response was significantly stronger during short fixations (two-tailed Wilcoxon signed rank tests, n = 128, z = 6.72, $P = 1.8 \times 10^{-11}$). *F*: same as *E*, but for 229 FEF neurons. Hundred and eighteen neurons (51.5%, red circles) had a significantly higher response during short fixations and nine neurons (3.8%, blue circles) had a significantly higher response during long fixations. The mean response was significantly stronger during short fixations (two-tailed Wilcoxon signed rank tests, n = 229, z = 10.55, $P = 5.19 \times 10^{-26}$). *G*: the responses of 200 LIP neurons in long fixation durations in ongoing search are compared to baseline activity. Total 137 (68.5%, red circles) responded significantly higher in ongoing search than in the baseline condition and nineteen neurons (9.5%, blue circles) responded significantly less (two-tailed t test, $P < 0.05$) during ongoing search. The mean response of the population was significantly higher during search than in the baseline condition (two-tailed Wilcoxon signed rank tests, n = 200, z = 9.58, $P = 9.4 \times 10^{-22}$). *H*: same as for *G*, but for 231 FEF neurons. Total 106 neurons (45.9%, red circles) responded significantly higher in ongoing search than in the baseline condition and 37 neurons (16.0%, blue circles) responded significantly less during ongoing search. The mean response of the population was significantly higher during search than in the baseline condition (two-tailed Wilcoxon signed rank tests, n = 231, z = 6.96, $P = 3.5 \times 10^{-12}$). FEF, frontal eye field; LIP, lateral intraparietal area.

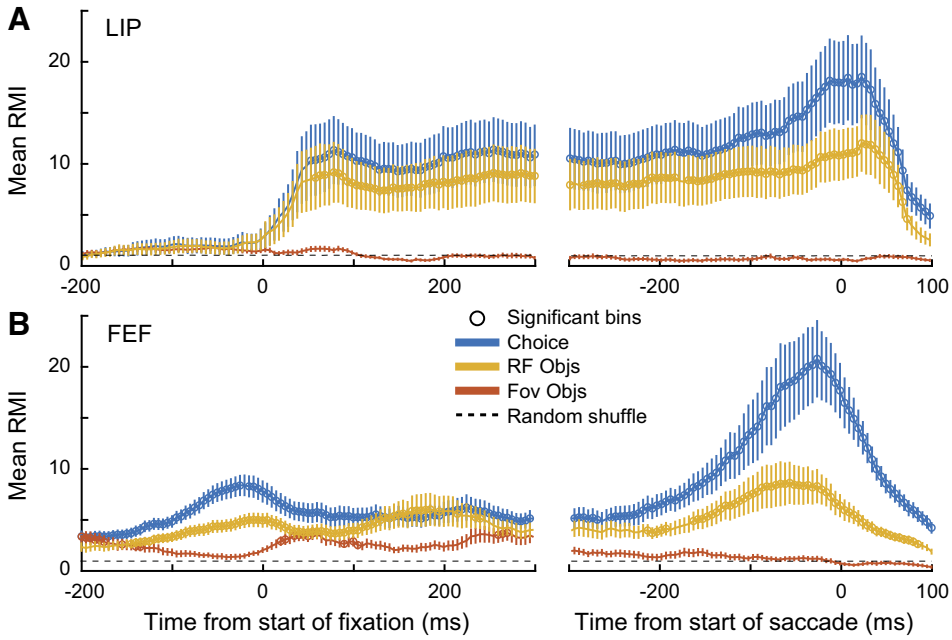

Figure 5. Mean response modulation index (RMI) of the population of LIP (*A*) and FEF (*B*) neurons during ongoing search aligned by start of fixation (*left*) and start of the next saccade (*right*). Blue traces represent behavioral choice (saccade to or away from RF), orange traces represent the identity of the object in the RF (targets or distractor), red traces represent the identity of the object at the fovea (target or distractor), and black dashed lines represent chance level, calculated by random shuffling. Significant bins are denoted by circles ($P < 0.005$, Wilcoxon Signed-rank tests). Error bars show SE across the population. FEF, frontal eye field; Fov, fovea; LIP, lateral intraparietal area; Objs, objects; RF, receptive field.

whereas in FEF, less than half (106/231) of the neurons responded significantly more than baseline (Fig. 4*H*) and 37/231 neurons (16.0%) had responses that were significantly less than baseline. As a result, the mean FEF response during maintained fixation was only 28% higher than baseline, whereas the mean LIP response was double that (58%). By comparison, the mean response in a 200-ms window before saccade onset for saccades made into the RF (blue traces in Fig. 3, *C* and *D*) was 90% higher than baseline in LIP and 94% higher than baseline in FEF, showing that the reduced response during maintained fixation represents a substantially stronger reduction in activity in FEF.

A third noticeable difference between the responses in LIP and FEF during ongoing search is the timing of the apparent burst of activity in each area. In LIP, we see a postsaccade enhancement in activity which begins just as the saccade ends and fixation begins (Fig. 3*C*). We have examined this in a subset of the neurons presented here previously and concluded this represents a postsaccade period of excitability, but one that aligns best with the start of the saccade (35). These dynamics are very different to those seen in FEF, which look more like the traditional build-up activity seen before saccade onset (Fig. 3*D*). However, it is important to reiterate that the target (green trace) and distractor (red trace) data presented in Fig. 3*D* only include fixations for saccades made away from the RF, so this ramping up of response is not the same as the movement response, which is shown in the blue trace. Instead, we suggest the apparent ramping up of the response when saccades were made away from the RF represents the release of the suppression seen during maintained fixation (31).

Modulation of Response and Response Modulation Index

Analyzing the average responses of the neurons to the objects inside the receptive field gives us a general sense of the response properties of the two areas. However, averaging out trial-to-trial fluctuations can potentially misrepresent the amount of information conveyed about factors by each neuron. Population modulation effects can also be averaged out in the simple statistical summarizations as the result of population diversity. Therefore, to measure the information carried about the behavioral parameters, we calculated an RMI, which is less prone to these weaknesses since it works based on the variance of the response, not the magnitude of it. RMI provides an explicit measure of the signal-to-noise ratio using *f* statistics (see METHODS). RMIs for each single neuron were calculated based on three parameters: RF object (whether there was an unfixated target or distractor in the RF), fovea object (whether there was a target or distractor on the fovea), and behavioral choice (whether the upcoming saccade was made to or away from the RF). Each was calculated as a function of the current and next fixations (see Fig. 1*B*).

During Ongoing Search, the RMI Pattern in LIP Is Stable, but Dynamic in FEF

In LIP, the RMI patterns for the RF object and saccade choice factors were relatively stable across fixations during ongoing search (Fig. 5*A*). These factors modulated the responses of LIP neurons soon after the start of the fixation and kept modulating it to the end of the fixation. This modulation was significant in most fixation time bins when compared to the shuffled RMI (circle markers in Fig. 5*A*). The modulation of response as a function of the stimulus at the fovea was at chance levels throughout the fixation (red trace in Fig. 5*A*). LIP neuronal responses were modulated within 50 ms of the start the fixation and the modulations were relatively stable until the next saccade was made, with a slight increase in the choice condition, starting ~50 ms before saccade onset. These patterns were typical at the single neuron level (Fig. 6, *A* and *B*).

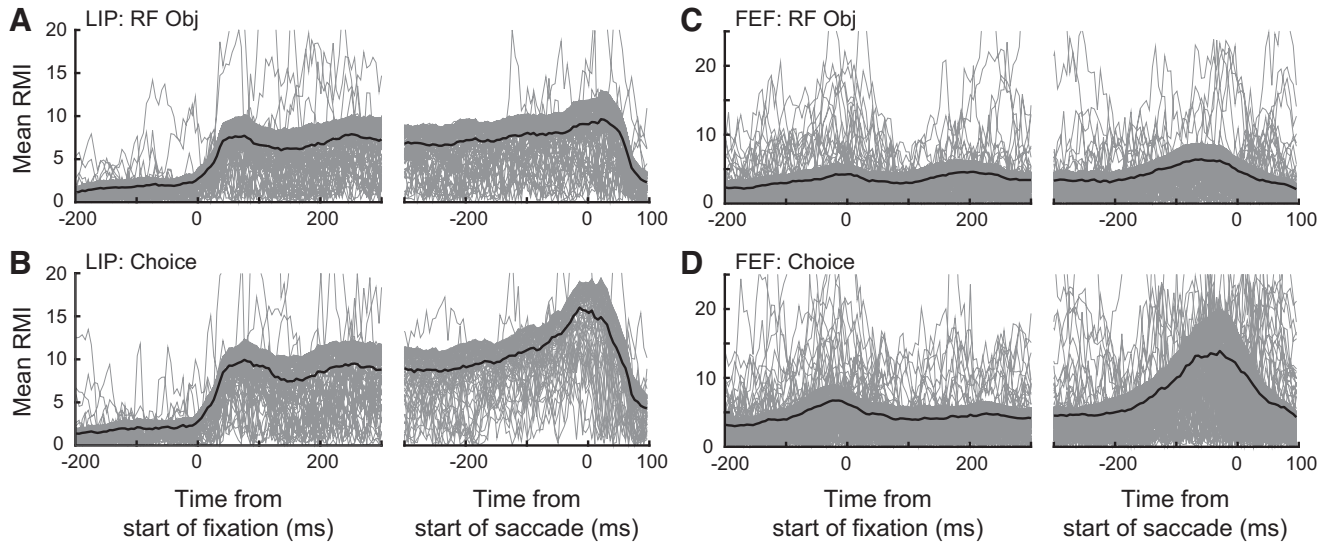

Figure 6. Response modulation index (RMI) from the single neurons. RMIs from LIP neurons for the RF object condition (*A*) and the choice condition (*B*). *Left* panels are aligned by the start of the fixation and the *right* panels are aligned by the start of the next saccade. The number of removed outliers from the population of 200 were 13 and 19 from the *left* and *right* panels, respectively, in *A* and 16 and 25, from the *left* and *right* panels, respectively, in *B*. RMIs from FEF neurons for the RF object condition (*C*) and the choice condition (*D*). *Left* panels are aligned by the start of the fixation and the *right* panels are aligned by the start of the next saccade. The number of removed outliers from the population of 231 were 24 and 27 from the *left* and *right* panels, respectively, in *C* and 28 and 25, from the *left* and *right* panels, respectively, in *D*. FEF, frontal eye field; LIP, lateral intraparietal area; Obj, object; RF, receptive field.

The pattern of RMI was noticeably different in FEF (Fig. 5*B*). Unlike LIP, FEF neurons were only weakly modulated during most of the fixation period and this modulation was only consistently significant in the choice condition. The modulation due to the identity of the stimulus in the RF was significant in the first 200 ms, but was not consistently significant again until ~180 ms before the upcoming saccade. Most notably, the strongest modulations in FEF occurred ~50 ms before the start of the next saccade as a function of the animals' choice, which followed a buildup of ~200 ms. Unlike LIP, these patterns of modulation did not appear to be consistent across all FEF neurons (Fig. 6, *C* and *D*).

To compare the consistency of the pattern of the modulation among the neurons, we calculated the first principal component of the RMI signals and the amount of variance it explained. In LIP, the first principal component for the choice and RF object factors built up ~50 ms after fixation onset and remained stable until the onset of the next saccade (Fig. 7*A*). In addition, the first principal component explained at least 90% of the RMI population variance for

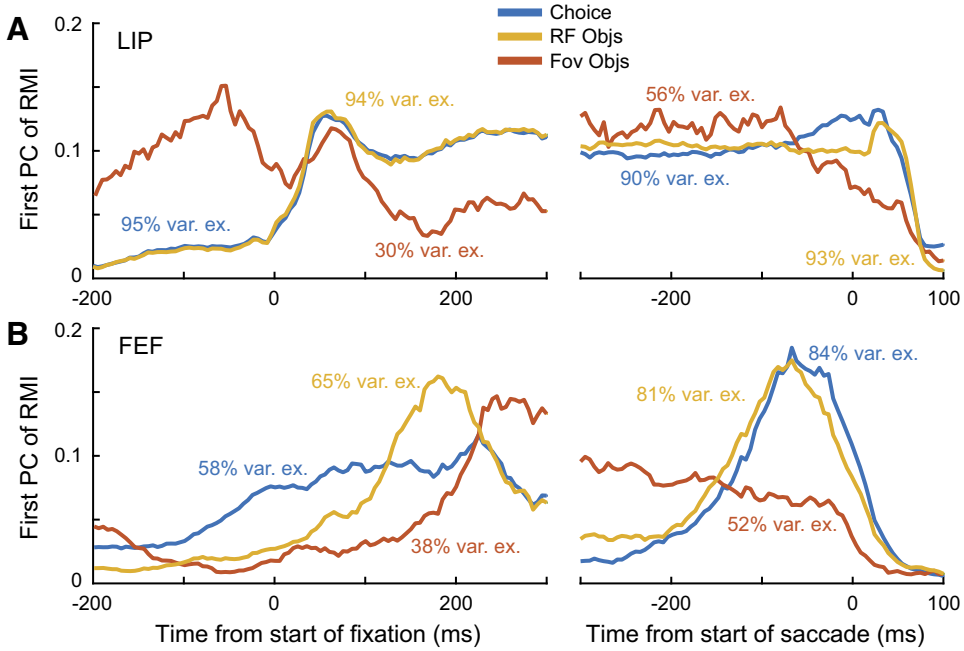

Figure 7. The first principal component (PC) of the RMI calculated by principal component analysis for the population of LIP (*A*) and FEF (*B*) neurons. Blue traces represent behavioral choice, orange traces represent the identity of the object in the receptive field (RF) and red traces represent the identity of the object at the fovea (Fov). The matching colored numbers show the amount of variance that was explained by the first PC. FEF, frontal eye field; LIP, lateral intraparietal area; Objs, objects; var. ex., variance explained.

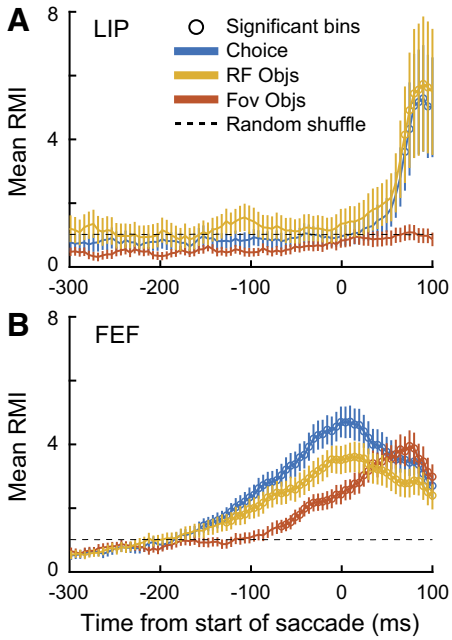

Figure 8. Mean RMIs calculated as a function of choice, fovea objects, or receptive field (RF) objects for the next fixation, aligned by the start of the next saccade for the population of LIP (*A*) and FEF (*B*) neurons. Blue traces represent behavioral choice (saccade to or away from RF), orange traces represent the identity of the object in the RF (targets or distractor), red traces represent the identity of the object at the fovea (target or distractor), and black dashed lines represent chance level, calculated by random shuffling. Significant bins are denoted by circles and error bars show SE across the population. FEF, frontal eye field; Fov, fovea; LIP, lateral intraparietal area; Objs, objects; RMI, response modulation index.

both factors in both epochs. This indicates that the choice and RF object factors consistently modulated the LIP neurons' responses and the cell-to-cell variance was low. The first principal component of the RMI for the fovea object factor was volatile and only explained 30% of the variance early in fixation and 56% of the variance late in fixation. This is likely due to the very weak RMI seen for this factor.

The FEF neurons showed less consistency in response modulation, except in the period just before the onset of the saccade. During fixation, the first principal component of the choice and RF object factors explained only 58% and 65% of the population variance, respectively. In the 200 ms leading up to saccade onset, both the first principal component and the percentage of the variance it explained increased for both factors (*right*, Fig. 7*B*). Like LIP, the first principal component of the RMI for the fovea object factor was weaker than for the other two factors, explaining only 38% of the variance early in fixation and 52% of the variance late in fixation. Note that because fixations lasted a minimum of 300 ms and were mostly longer than 600 ms, the apparent peak in the RF object data in Fig. 7*B, left*, which represents only 65% of the variance, is unrelated to the peak in the Fig. 7*B, right*, which represents over 80% of the variance.

So far, we have analyzed the effect of the parameters of the current fixation using the response of the current fixation. However, the effect of factors might not be restricted to the current fixation, as seen by the number of significant RMI bins in Fig. 5*B* before the start of fixation. Given that the neuronal responses of FEF neurons tend to show a buildup that is better aligned to the start of the saccade than to the start of fixation, we looked at the response modulation before the saccade based on factors in next the fixation, aligned by saccade onset (Fig. 8). There was no predictive modulation before saccade onset in LIP (Fig. 8*A*), but there was a clear buildup in FEF (Fig. 8*B*). FEF neurons were modulated by the choice of the next saccade (not the saccade made at this time) starting ~150 ms before saccade onset and by both the identity of the RF objects, starting ~150 ms before saccade onset, and the identity of the object at the fovea starting less than 100 ms before saccade onset. Note that the scale is different to that in Fig. 5, indicating that the overall strength of these modulations is relatively weak compared to the modulations driven by the choice for the current saccade (right panel, Fig. 5*B*).

To summarize the RMI results, LIP neurons showed a representation of the identity of the stimulus in the RF and the saccade goal from the start of fixation to its end. This representation was consistent across the population and relatively stable across time. On the other hand, FEF neurons were not modulated as strongly as LIP neurons during fixation, but the modulation started to rise and became consistent in the population ~200 ms before the start of the upcoming saccade.

Comodulation as a Measure of Priority

RMI values give us a good indication of the stimulus and choice information in LIP and FEF, however it is not clear how much the stimulus representations contribute to the choice. To test this, we performed a comodulation analysis between the choice RMI and each of the two stimulus RMIs (the identity of the stimulus in the RF or the identity of the stimulus at the fovea). The comodulation value was calculated by multiplying the RF object or the fovea object RMI by the choice RMI and then averaging them across the population. The final value can be interpreted as a population covariance of the combined main effects. To find chance level, the comodulation was calculated for shuffled RMIs (see METHODS for details). Because a priority map can be defined as the integration of sensory and task relevant signals used to guide behavior, we suggest that the comodulation of the stimulus and choice signals can be considered as a metric of priority.

The normalized population comodulation values for the RF object and choice (orange trace) and for the foveal object and choice (red trace) are shown in Fig. 9. In LIP, the choice RMI comodulated with the RF object RMI for the duration of fixation (Fig. 9*A*). Shortly after fixation onset, it rose to a significant level (circles) and stayed high during the rest of the fixation, with a slight enhancement beginning ~50 ms before the start of the saccade. This means that the modulation of LIP activity represents not only the identity of the stimulus in the RF, but how it will guide the upcoming choice of saccade goal. There was no significant comodulation between the foveal object RMI and choice at any time.

In FEF, the comodulation between the RF object RMI and choice didn't show consistent or robust levels during maintained fixation, but it ramped up strongly around 200 ms before the start of the saccade (Fig. 9*B*). This suggests that

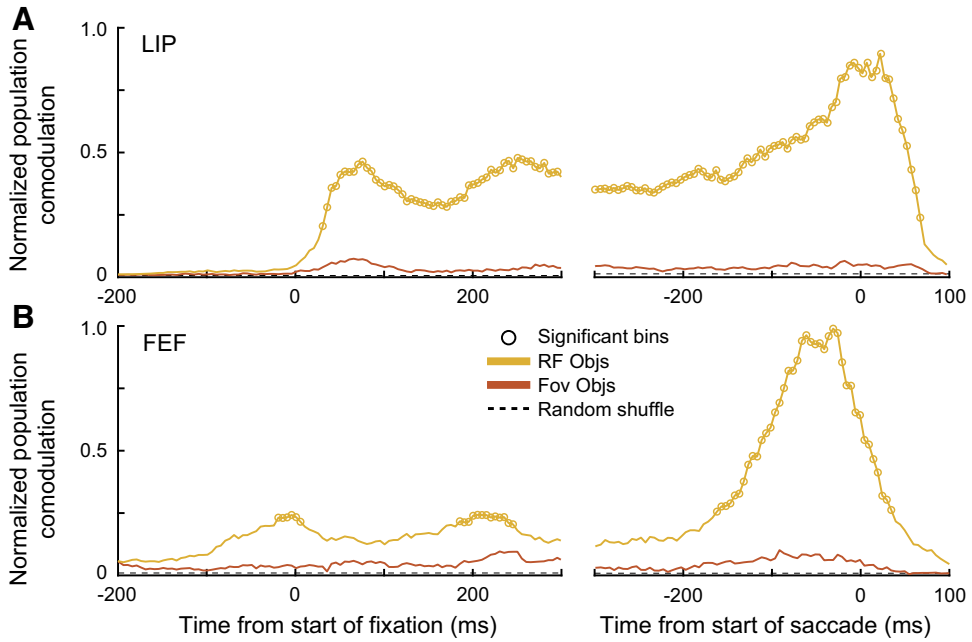

Figure 9. Normalized comodulation indices for the LIP (*A*) and FEF (*B*) neuronal populations, aligned by the start of the fixation (*left*) and by the start of the next saccade (*right*). Orange traces represent the comodulation of the receptive field (RF) object and behavioral choice, red traces represent the comodulation of the fovea objects and behavioral choice, and the black dashed lines represent chance level, calculated by random shuffling. Significant bins ($P < 0.005$, t test) are denoted by circles. FEF, frontal eye field; Fov, fovea; LIP, lateral intraparietal area; Objs, objects; RF, receptive field.

the choice signal that was consistent in FEF (Fig. 5*B*) was not driven by the identity of the stimulus in the RF until shortly before saccade onset. Like LIP, we found no significant or substantial comodulation between the foveal object RMI and choice at any time. This comodulation analysis indicates that the LIP priority representation is a stable and bound to the current fixation, while the FEF priority representation is dynamic, with a strong increase right before an eye movement.

Temporal Comodulation

In the previous section, we hypothesized that the LIP priority representation, as measured by comodulation, is stable over time because the comodulation metric remained at a somewhat similar level during stable fixation. To test this hypothesis, we created temporal comodulation maps for LIP and FEF, in which the comodulation of the RF object RMIs and the choice RMIs were compared across all possible combinations of times relative to fixation onset (Fig. 10). On these maps, the color of the points shows the normalized comodulation and significant points or groups of points are outlined by the red boundaries.

The LIP temporal comodulation map showed a block of high values starting ~50 ms after fixation onset along both dimensions (Fig. 10*A*). This means that, in this block, the RMI for one factor correlated with the RMI for the other factor, independent of the time each factor was tested. This shows that the representation of priority in LIP truly is stable over time.

The FEF temporal comodulation map (Fig. 10*B*) differed from the LIP comodulation map in three important ways. First, although LIP showed strongest comodulation during maintained fixation (i.e., after fixation onset along both dimensions), the strongest comodulation in FEF occurred close to the time of fixation onset. Note that this is aligned by the start of fixation (as in the *left* panel of Fig. 9*B*) and not by saccade onset (as in the *right* panel of Fig. 9*B*), so this is not the large saccade-related comodulation. Instead, it

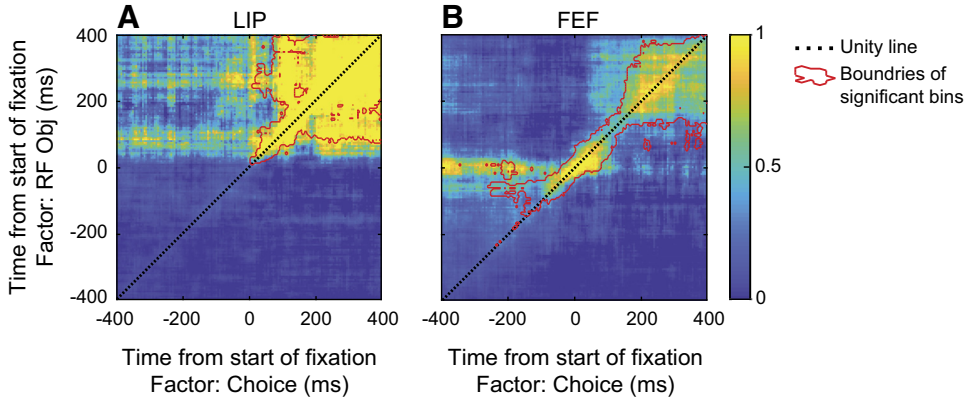

Figure 10. Temporal normalized comodulation plots for the LIP (*A*) and FEF (*B*) neuronal populations. Each epoch of the map was calculated based on the population comodulation of the receptive field (RF) object and the behavioral choice at a given pair of times. The red contour line shows the boundary of the significant epochs. The unity line is plotted in black dotted line. FEF, frontal eye field; LIP, lateral intraparietal area; Obj, object; RF, receptive field.

highlights how little consistent comodulation is present during maintained fixation in FEF. Second, most comodulation in FEF was found close to the diagonal, with the exception of some moderate comodulation found later in fixation. This means that FEF modulations do not show the sort of temporal stability seen in LIP. Finally, as implied in Figs. 5 and 8, FEF RMIs showed comodulation between the RF object and the upcoming saccade before fixation even began, whereas in LIP this only occurred after fixation onset.

DISCUSSION

Our data revealed representations of stimuli and choice in both FEF and LIP, but identified clear differences in the dynamics of the representations during maintained fixation in ongoing search. LIP and FEF neurons showed somewhat similar patterns of responses following array onset and responses in both areas were not modulated by the identity of the stimulus at the fovea at any time. During ongoing search, LIP neurons continued to discriminate targets and distractors consistently, whereas during long fixations FEF neurons were only modulated around the time of a saccade, with a large diversity of patterns in the population. And although the LIP representation was consistent within and constrained to each fixation, the FEF representation started before saccade onset. Based on these results, we suggest there is a more clearly defined division of labor within the cortical oculomotor circuit than previously thought: LIP provides a stable map of priority based on current information, while the FEF map is dynamic, represents additional information and only integrates it with current information to decide where to move the eye just before the eye movement is made.

We propose that, during free viewing search, LIP activity creates a simple map of visual space in which activity represents the behavioral importance of objects or locations in space and that this map is used to guide behavior. From previous work, we know that LIP activity is driven by low level salience (9) and a host of top-down factors, which can include reward expectation (14, 45–47), the similarity of a stimulus to a defined target (7, 22, 25, 48–51) or category (52, 53), inhibition of return (22), behavioral state (54), and gains in information not directly linked to a reward (55, 56). The present work adds to this by indicating that activity modulation in LIP is tied to the current fixation, is maintained throughout the fixation, is robust across the population and explains the resultant behavioral choice. To be clear, we are not suggesting that LIP makes the choice or that it converts the sensory and task-related data into a movement signal, instead we propose that it is a simple map that provides information about the attentional priority of the visual scene and, given the results of the comodulation analyses, it is likely that this activity is then used to guide behavior.

Even though predictive remapping has been seen in LIP (57), including in a subset of the neurons analyzed here using this task (33, 35), we found no indication of a predictive RMI signal in LIP. This suggests that the predictive signal may not be critical in the behavior of this task, and is consistent with our previous hypothesis that remapping in LIP may play a role in maintaining spatial stability across saccades (35, 58). Because the LIP activity is stable and temporally independent, as shown in Fig. 10, we conclude that the critical information represented in LIP is the behavioral relevance, represented in the magnitude of the response, and the spatial location, represented by which neurons are active.

The role of FEF in free viewing search behavior is more complex, both in terms of the consistency of responses within the area (as in Fig. 7*B*) and in terms of what and when information is processed. We cannot know all the factors that drive each animals' behavior: clearly they include information about the stimuli and the task, which we have defined as priority and which is consistently represented in LIP, but other factors may play a role, such as a bias to not revisit stimuli that have been examined earlier in the trial (59), a bias to search in a particular direction (60), a bias to move away from the edges (27), or even a strategic plan to make a series of saccades in a row (28). It has been suggested that many of these factors can be thought of as priors in a Bayesian framework (27). In this framework, visual information from the current fixation, that is, the activity in LIP, represents the likelihood, and this is combined with the priors in FEF to decide where to look next.

In this study, we found evidence that FEF plays a role in processing these other factors. When looking at the RMIs, we found a robust modulation of FEF activity based on saccade choice, which began even before saccade onset, and fluctuating modulation based on the identity of the object in the RF. Yet the comodulation of these factors was only consistently significant just before saccade onset. This suggests that the early choice modulation likely represents nonstimulus related factors that influence the choice. Indeed, this was seen even before fixation onset, which may use the remapping mechanism known to exist in FEF neurons (61) and is consistent with the idea that it could represent a strategic plan to make several eye movements in a row (28) or a bias in saccadic direction (27). In addition, we have previously shown that a subset of the FEF neurons analyzed here preferentially respond to a stimulus that has been fixated earlier in the trial (30) and that this signal is predictively remapped before each eye movement. Together, these data are consistent with the idea that FEF activity represents factors beyond just representing the identity of the stimulus in the RF or basic task rules. Whether these signals primarily reside in FEF, despite the low firing rate, as may be inferred by the consistent choice RMI throughout each fixation, or whether FEF is part of a broader network that processes such priors (62) is unclear from our data.

Although FEF carried some information about the identity of the stimulus in the RF, this was not represented in the comodulation during maintained fixation. This suggests that the stimulus representation in FEF early in the fixation did not affect the final choice, unlike in LIP, and that the emergence of the robust comodulation in FEF at the time of the saccade is driven by a signal from outside of FEF. Although we did not record from neurons in both areas simultaneously, given the connections between LIP and FEF and the fact that the signal was present in LIP, we suggest that LIP could be the source of this information. Overall, our data suggest that FEF activity is modulated by more complex task and non-task related factors that influence behavior, that when it is time to make the saccade, FEF activity can access

the LIP representation and that whatever controls the suppression in FEF, likely controls the temporal rhythm of the saccadic behavior. In the Bayesian framework, this suggests that LIP provides the likelihood, FEF provides the priors and then combines them to make the decision about where to look.

A key reason that we were able to identify these separable roles is that we used a behavioral task in which the animals had no oculomotor restrictions and made multiple eye movements on each trial. Many previous studies have examined the responses of LIP and FEF using single saccade, center-out visual search (e.g., 10, 50). These studies likely did not identify the differences we have shown here because, as we found ourselves, the responses immediately after array onset are very similar in the two areas.

Several previous studies have examined single and multiunit responses to task-relevant and task-irrelevant features in free viewing conjunction search. Whether using a task that required visually searching among many stimuli (51) or a center-out search task that did not punish incorrect saccades (25), both studies found that FEF activity was modulated by stimuli that shared features with the target, that this modulation occurred during ongoing search and that this modulation emerged at the same time in LIP, albeit less robustly than in FEF. Our task was not designed to look at feature modulation beyond the basic distinction between the potentially rewarding Ts and task-irrelevant distractors, which remained consistent across tens of thousands of trials. As such, the robust modulation we saw in LIP may be a product of training (63) and may overemphasize the feature coding in this area compared to when targets can change on a trial-by-trial bases in conjunction search (25). Likewise, by design, our task encourages the animals to pause search by fixating potential targets. These pauses mimic the longer fixation durations that can occur in natural reading and scene perception (64) and that are the reason for the inhibition seen in models of eye movement behavior in search (65, 66), scene perception (67, 68), and reading (69, 70). When we examined short duration fixations, we also found elevated activity throughout the fixation (see Fig. 4, *E* and *F*), suggesting that the lack of signal in longer durations is likely due to the overall reduction in response (31). Indeed, with fixation durations under 200 ms, the integration we see emerging late in long fixations is likely to occur immediately. So although our data are unable to address the flow of information in these cases, they clearly show that FEF signals during maintained fixation are not sufficient to guide eye movements and that these signals must come from elsewhere. Given the natural disposition animals have in performing this task (training of a naïve animal typically takes 4–6 wk), we believe these results reflect an inherent mechanism rather than a product of training.

The interpretation we present here pertains to eye movement decisions, but both FEF (3, 60, 71) and LIP (1, 72–75) are known to play a role in guiding covert attention. Indeed, FEF neurons maintain robust activity during maintained fixation in visual search tasks, best illustrated in the accurate trials in speed accuracy tradeoff studies (76, 77). The data we present from the memory-guided saccade task (Fig. 2) showed that the population of FEF neurons we recorded from has elevated activity during the delay, yet the mean response of the same population of neurons dropped to or below baseline after 150–200 ms in the foraging task (Fig. 3*D*). This indicates that the activity in FEF is different depending on whether animals are performing naturalistic free viewing eye movements or a covert attention task. We interpret this to mean that these represent two different states within the network.

Our view is that in the natural viewing state, as mimicked in our task, the main role of FEF is to affect the timing of saccades and to integrate longer-term biases or priors. In covert attention tasks, in which the eye is not allowed to move or in which only one eye movement is allowed, but in which wrong saccades are punished (such as in the memory-guided saccade task), the temporal dynamics of an animal's behavior is dictated by the rules of the task: either go at a signal or do not go unless you are sure. We speculate that in this state, the primary role of FEF is to drive top-down attentional effects in visual areas, to allow the brain to continuously update visual information pertinent to the task. In the case of the memory guided saccade, this would be the persistent activity at the target/saccade goal location, which is necessary for a robust representation of the same signal in LIP (78). Given the importance of FEF activity in these tasks, the sort of suppression seen in free viewing would be counterproductive.

Although speculative, our hypothesis makes a concrete prediction: while performing a free viewing behavior, covert spatial attention benefits, such as shortened reaction times (79) or enhanced sensitivity (80, 81), should not be active, even during maintained fixation. Note that in the memory-guided saccade, attentional benefits are seen at the target/saccade goal location during the delay (1, 82), consistent with our hypothesis.

In summary, our results support the hypothesis that in free viewing oculomotor behavior, LIP provides a stable map of priority based on current information, while FEF is dynamic, representing more complex information, including biases and priors. When an eye movement is to be made, FEF integrates all these signals to decide where to move the eye next.

ACKNOWLEDGMENTS

We thank members of the University of California, Los Angeles Department of Animal Laboratory Medicine for their superb animal care and to Drs. Fabrice Arcizet, Wei Song Ong, and Zeinab Bolandnazar for help in recording the data presented here.

GRANTS

This work was supported by the National Eye Institute Grants R01 EY019273 and R01 EY027968.

DISCLOSURES

No conflicts of interest, financial or otherwise, are declared by the authors.

AUTHOR CONTRIBUTIONS

K.M. and J.W.B. conceived and designed research; K.M. performed experiments; K.M. and J.W.B. analyzed data; K.M. and J.W.B. interpreted results of experiments; K.M. and J.W.B. prepared figures; K.M. and J.W.B. drafted manuscript; K.M. and J.W.B.

edited and revised manuscript; K.M. and J.W.B. approved final version of manuscript.

REFERENCES

1. **Bisley JW**, **Goldberg ME.** Neuronal activity in the lateral intraparietal area and spatial attention. *Science* 299: 81–86, 2003. doi:10.1126/science.1077395.
2. **Herrington TM**, **Assad JA.** Neural activity in the middle temporal area and lateral intraparietal area during endogenously cued shifts of attention. *J Neurosci* 29: 14160–14176, 2009. doi:10.1523/JNEUROSCI.1916-09.2009.
3. **Moore T**, **Fallah M.** Control of eye movements and spatial attention. *Proc Natl Acad Sci USA* 98: 1273–1276, 2001. doi:10.1073/pnas.021549498.
4. **Moore T**, **Fallah M.** Microstimulation of the frontal eye field and its effects on covert spatial attention. *J Neurophysiol* 91: 152–162, 2004. doi:10.1152/jn.00741.2002.
5. **Barash S**, **Bracewell RM**, **Fogassi L**, **Gnadt JW**, **Andersen RA.** Saccade-related activity in the lateral intraparietal area. I. Temporal properties; comparison with area 7a. *J Neurophysiol* 66: 1095–1108, 1991. doi:10.1152/jn.1991.66.3.1095.
6. **Bruce CJ**, **Goldberg ME.** Primate frontal eye fields. I. Single neurons discharging before saccades. *J Neurophysiol* 53: 603–635, 1985. doi:10.1152/jn.1985.53.3.603.
7. **Ipata AE**, **Gee AL**, **Goldberg ME**, **Bisley JW.** Activity in the lateral intraparietal area predicts the goal and latency of saccades in a free-viewing visual search task. *J Neurosci* 26: 3656–3661, 2006. doi:10.1523/JNEUROSCI.5074-05.2006.
8. **Robinson DA**, **Fuchs AF.** Eye movements evoked by stimulation of frontal eye fields. *J Neurophysiol* 32: 637–648, 1969. doi:10.1152/jn.1969.32.5.637.
9. **Arcizet F**, **Mirpour K**, **Bisley JW.** A pure salience response in posterior parietal cortex. *Cereb Cortex* 21: 2498–2506, 2011. doi:10.1093/cercor/bhr035.
10. **Thompson KG**, **Hanes DP**, **Bichot NP**, **Schall JD.** Perceptual and motor processing stages identified in the activity of macaque frontal eye field neurons during visual search. *J Neurophysiol* 76: 4040–4055, 1996. doi:10.1152/jn.1996.76.6.4040.
11. **Buschman TJ**, **Miller EK.** Top-down versus bottom-up control of attention in the prefrontal and posterior parietal cortices. *Science* 315: 1860–1862, 2007. doi:10.1126/science.1138071.
12. **Ding L**, **Gold JI.** Neural correlates of perceptual decision making before, during, and after decision commitment in monkey frontal eye field. *Cereb Cortex* 22: 1052–1067, 2012. doi:10.1093/cercor/bhr178.
13. **Gottlieb JP**, **Kusunoki M**, **Goldberg ME.** The representation of visual salience in monkey parietal cortex. *Nature* 391: 481–484, 1998. doi:10.1038/35135.
14. **Platt ML**, **Glimcher PW.** Neural correlates of decision variables in parietal cortex. *Nature* 400: 233–238, 1999. doi:10.1038/22268.
15. **Gnadt JW**, **Andersen RA.** Memory related motor planning activity in posterior parietal cortex of macaque. *Exp Brain Res* 70: 216–220, 1988. doi:10.1007/BF00271862.
16. **Bruce CJ**, **Goldberg ME**, **Bushnell MC**, **Stanton GB.** Primate frontal eye fields. II. Physiological and anatomical correlates of electrically evoked eye movements. *J Neurophysiol* 54: 714–734, 1985. doi:10.1152/jn.1985.54.3.714.
17. **Shibutani H**, **Sakata H**, **Hyvarinen J.** Saccade and blinking evoked by microstimulation of the posterior parietal association cortex of the monkey. *Exp Brain Res* 55: 1–8, 1984. doi:10.1007/BF00240493.
18. **Constantin AG**, **Wang H**, **Martinez-Trujillo JC**, **Crawford JD.** Frames of reference for gaze saccades evoked during stimulation of lateral intraparietal cortex. *J Neurophysiol* 98: 696–709, 2007. doi:10.1152/jn.00206.2007.
19. **Thier P**, **Andersen RA.** Electrical microstimulation distinguishes distinct saccade-related areas in the posterior parietal cortex. *J Neurophysiol* 80: 1713–1735, 1998. doi:10.1152/jn.1998.80.4.1713.
20. **Itti L**, **Koch C.** Computational modelling of visual attention. *Nat Rev Neurosci* 2: 194–203, 2001. doi:10.1038/35058500.
21. **Zelinsky GJ**, **Bisley JW.** The what, where, and why of priority maps and their interactions with visual working memory. *Ann NY Acad Sci* 1339: 154–164, 2015. doi:10.1111/nyas.12606.
22. **Mirpour K**, **Arcizet F**, **Ong WS**, **Bisley JW.** Been there, seen that: a neural mechanism for performing efficient visual search. *J Neurophysiol* 102: 3481–3491, 2009. doi:10.1152/jn.00688.2009.
23. **Thompson KG**, **Bichot NP.** A visual salience map in the primate frontal eye field. *Prog Brain Res* 147: 251–262, 2005. doi:10.1016/S0079-6123(04)47019-8.
24. **Ibos G**, **Duhamel JR**, **Ben Hamed S.** A functional hierarchy within the parietofrontal network in stimulus selection and attention control. *J Neurosci* 33: 8359–8369, 2013. doi:10.1523/JNEUROSCI.4058-12.2013.
25. **Sapountzis P**, **Paneri S**, **Gregoriou GG.** Distinct roles of prefrontal and parietal areas in the encoding of attentional priority. *Proc Natl Acad Sci USA* 115: E8755–E8764, 2018. doi:10.1073/pnas.1804643115.
26. **Burman DD**, **Segraves MA.** Primate frontal eye field activity during natural scanning eye movements. *J Neurophysiol* 71: 1266–1271, 1994. doi:10.1152/jn.1994.71.3.1266.
27. **Glaser JI**, **Wood DK**, **Lawlor PN**, **Segraves MA**, **Kording KP.** From prior information to saccade selection: evolution of frontal eye field activity during natural scene search. *Cereb Cortex* 30: 1957–1973, 2020. doi:10.1093/cercor/bhz216.
28. **Phillips AN**, **Segraves MA.** Predictive activity in macaque frontal eye field neurons during natural scene searching. *J Neurophysiol* 103: 1238–1252, 2010. doi:10.1152/jn.00776.2009.
29. **Mirpour K**, **Bisley JW.** Dissociating activity in the lateral intraparietal area from value using a visual foraging task. *Proc Natl Acad Sci USA* 109: 10083–10088, 2012. doi:10.1073/pnas.1120763109.
30. **Mirpour K**, **Bolandnazar Z**, **Bisley JW.** Neurons in FEF keep track of items that have been previously fixated in free viewing visual search. *J Neurosci* 39: 2114–2124, 2019. doi:10.1523/JNEUROSCI.1767-18.2018.
31. **Mirpour K**, **Bolandnazar Z**, **Bisley JW.** Suppression of frontal eye field neuronal responses with maintained fixation. *Proc Natl Acad Sci USA* 115: 804–809, 2018. doi:10.1073/pnas.1716315115.
32. **Bisley JW**, **Mirpour K.** The neural instantiation of a priority map. *Curr Opin Psychol* 29: 108–112, 2019. doi:10.1016/j.copsyc.2019.01.002.
33. **Mirpour K**, **Bisley JW.** Anticipatory remapping of attentional priority across the entire visual field. *J Neurosci* 32: 16449–16457, 2012. doi:10.1523/JNEUROSCI.2008-12.2012.
34. **Mirpour K**, **Bisley JW.** Evidence for differential top-down and bottom-up suppression in posterior parietal cortex. *Philos Trans R Soc Lond B Biol Sci* 368: 20130069, 2013. doi:10.1098/rstb.2013.0069.
35. **Mirpour K**, **Bisley JW.** Remapping, spatial stability, and temporal continuity: from the pre-saccadic to postsaccadic representation of visual space in LIP. *Cereb Cortex* 26: 3183–3195, 2016. doi:10.1093/cercor/bhv153.
36. **Hays AV**, **Richmond BJ**, **Optican LM.** Unix-based multiple-process system, for real-time data acquisition and control. *WESCON Conf Proc* 2: 1–10, 1982. [www.osti.gov/biblio/5213621]
37. **Sommer MA**, **Wurtz RH.** Composition and topographic organization of signals sent from the frontal eye field to the superior colliculus. *J Neurophysiol* 83: 1979–2001, 2000. doi:10.1152/jn.2000.83.4.1979.
38. **Bizzi E.** Discharge of frontal eye field neurons during saccadic and following eye movements in unanesthetized monkeys. *Exp Brain Res* 6: 69–80, 1968. doi:10.1007/BF00235447.
39. **Suzuki H**, **Azuma M.** Prefrontal neuronal activity during gazing at a light spot in the monkey. *Brain Res* 126: 497–508, 1977. doi:10.1016/0006-8993(77)90600-X.
40. **Mirpour K**, **Ong WS**, **Bisley JW.** Microstimulation of posterior parietal cortex biases the selection of eye movement goals during search. *J Neurophysiol* 104: 3021–3028, 2010. doi:10.1152/jn.00397.2010.
41. **Richmond BJ**, **Optican LM**, **Podell M**, **Spitzer H.** Temporal encoding of two-dimensional patterns by single units in primate inferior temporal cortex. I. Response characteristics. *J Neurophysiol* 57: 132–146, 1987. doi:10.1152/jn.1987.57.1.132.
42. **Hegde J**, **Van Essen DC.** Temporal dynamics of 2D and 3D shape representation in macaque visual area V4. *Vis Neurosci* 23: 749–763, 2006. doi:10.1017/S0952523806230074.
43. **Hegde J**, **Van Essen DC.** Temporal dynamics of shape analysis in macaque visual area V2. *J Neurophysiol* 92: 3030–3042, 2004. doi:10.1152/jn.00822.2003.
44. **Leys C**, **Ley C**, **Klein O**, **Bernard P**, **Licata L.** Detecting outliers: do not use standard deviation around the mean, use absolute deviation

around the median. *J Exp Soc Psychol* 49: 764–766, 2013. doi:10.1016/j.jesp.2013.03.013.
45. **Dorris MC**, **Glimcher PW.** Activity in posterior parietal cortex is correlated with the relative subjective desirability of action. *Neuron* 44: 365–378, 2004. doi:10.1016/j.neuron.2004.09.009.
46. **Louie K**, **Glimcher PW.** Separating value from choice: delay discounting activity in the lateral intraparietal area. *J Neurosci* 30: 5498–5507, 2010. doi:10.1523/JNEUROSCI.5742-09.2010.
47. **Sugrue LP**, **Corrado GS**, **Newsome WT.** Matching behavior and the representation of value in the parietal cortex. *Science* 304: 1782–1787, 2004. doi:10.1126/science.1094765.
48. **Ogawa T**, **Komatsu H.** Condition-dependent and condition-independent target selection in the macaque posterior parietal cortex. *J Neurophysiol* 101: 721–736, 2009. doi:10.1152/jn.90817.2008.
49. **Ong WS**, **Mirpour K**, **Bisley JW.** Object comparison in the lateral intraparietal area. *J Neurophysiol* 118: 2458–2469, 2017. doi:10.1152/jn.00400.2017.
50. **Thomas NW**, **Pare M.** Temporal processing of saccade targets in parietal cortex area LIP during visual search. *J Neurophysiol* 97: 942–947, 2007. doi:10.1152/jn.00413.2006.
51. **Zhou H**, **Desimone R.** Feature-based attention in the frontal eye field and area V4 during visual search. *Neuron* 70: 1205–1217, 2011. doi:10.1016/j.neuron.2011.04.032.
52. **Freedman DJ**, **Assad JA.** Experience-dependent representation of visual categories in parietal cortex. *Nature* 443: 85–88, 2006. doi:10.1038/nature05078.
53. **Swaminathan SK**, **Freedman DJ.** Preferential encoding of visual categories in parietal cortex compared with prefrontal cortex. *Nat Neurosci* 15: 315–320, 2012. doi:10.1038/nn.3016.
54. **Zhang M**, **Wang X**, **Goldberg ME.** A spatially nonselective baseline signal in parietal cortex reflects the probability of a monkey's success on the current trial. *Proc Natl Acad Sci USA* 111: 8967–8972, 2014. doi:10.1073/pnas.1407540111.
55. **Foley NC**, **Kelly SP**, **Mhatre H**, **Lopes M**, **Gottlieb J.** Parietal neurons encode expected gains in instrumental information. *Proc Natl Acad Sci USA* 114: E3315–E3323, 2017. doi:10.1073/pnas.1613844114.
56. **Horan M**, **Daddaoua N**, **Gottlieb J.** Parietal neurons encode information sampling based on decision uncertainty. *Nat Neurosci* 22: 1327–1335, 2019. doi:10.1038/s41593-019-0440-1.
57. **Duhamel JR**, **Colby CL**, **Goldberg ME.** The updating of the representation of visual space in parietal cortex by intended eye movements. *Science* 255: 90–92, 1992. doi:10.1126/science.1553535.
58. **Bisley JW**, **Mirpour K**, **Alkan Y.** The functional roles of neural remapping in cortex. *J Vis* 20: 6, 2020. doi:10.1167/jov.20.9.6.
59. **Klein R.** Inhibitory tagging system facilitates visual search. *Nature* 334: 430–431, 1988. doi:10.1038/334430a0.
60. **Buschman TJ**, **Miller EK.** Serial, covert shifts of attention during visual search are reflected by the frontal eye fields and correlated with population oscillations. *Neuron* 63: 386–396, 2009. doi:10.1016/j.neuron.2009.06.020.
61. **Umeno MM**, **Goldberg ME.** Spatial processing in the monkey frontal eye field. I. Predictive visual responses. *J Neurophysiol* 78: 1373–1383, 1997. doi:10.1152/jn.1997.78.3.1373.
62. **Sohn H**, **Narain D**, **Meirhaeghe N**, **Jazayeri M.** Bayesian computation through cortical latent dynamics. *Neuron* 103: 934–947.e5, 2019. doi:10.1016/j.neuron.2019.06.012.
63. **Sarma A**, **Masse NY**, **Wang XJ**, **Freedman DJ.** Task-specific versus generalized mnemonic representations in parietal and prefrontal cortices. *Nat Neurosci* 19: 143–149, 2016. doi:10.1038/nn.4168.
64. **Rayner K**, **Castelhano MS.** Eye movements during reading, scene perception, visual search, and while looking at print advertisements. In: *Visual Marketing: From Attention to Action*, edited by Wedel P, Pieters R. Hillsdale, NJ: Erlbaum, 2007, p. 942.
65. **Godwin HJ**, **Reichle ED**, **Menneer T.** Modeling lag-2 revisits to understand trade-offs in mixed control of fixation termination during visual search. *Cogn Sci* 41: 996–1019, 2017. doi:10.1111/cogs.12379.
66. **Trukenbrod HA**, **Engbert R.** ICAT: a computational model for the adaptive control of fixation durations. *Psychon Bull Rev* 21: 907–934, 2014. doi:10.3758/s13423-013-0575-0.
67. **Nuthmann A**, **Smith TJ**, **Engbert R**, **Henderson JM.** CRISP: a computational model of fixation durations in scene viewing. *Psychol Rev* 117: 382–405, 2010. doi:10.1037/a0018924.
68. **Tatler BW**, **Brockmole JR**, **Carpenter RH.** LATEST: a model of saccadic decisions in space and time. *Psychol Rev* 124: 267–300, 2017. doi:10.1037/rev0000054.
69. **Engbert R**, **Nuthmann A**, **Richter EM**, **Kliegl R.** SWIFT: a dynamical model of saccade generation during reading. *Psychol Rev* 112: 777–813, 2005. doi:10.1037/0033-295X.112.4.777.
70. **Reichle ED**, **Pollatsek A**, **Fisher DL**, **Rayner K.** Toward a model of eye movement control in reading. *Psychol Rev* 105: 125–157, 1998. doi:10.1037/0033-295x.105.1.125.
71. **Wardak C**, **Ibos G**, **Duhamel JR**, **Olivier E.** Contribution of the monkey frontal eye field to covert visual attention. *J Neurosci* 26: 4228–4235, 2006. doi:10.1523/JNEUROSCI.3336-05.2006.
72. **Balan PF**, **Gottlieb J.** Functional significance of nonspatial information in monkey lateral intraparietal area. *J Neurosci* 29: 8166–8176, 2009. doi:10.1523/JNEUROSCI.0243-09.2009.
73. **Cutrell EB**, **Marrocco RT.** Electrical microstimulation of primate posterior parietal cortex initiates orienting and alerting components of covert attention. *Exp Brain Res* 144: 103–113, 2002. doi:10.1007/s00221-002-1032-x.
74. **Davidson MC**, **Marrocco RT.** Local infusion of scopolamine into intraparietal cortex slows covert orienting in rhesus monkeys. *J Neurophysiol* 83: 1536–1549, 2000. doi:10.1152/jn.2000.83.3.1536.
75. **Liu Y**, **Yttri EA**, **Snyder LH.** Intention and attention: different functional roles for LIPd and LIPv. *Nat Neurosci* 13: 495–500, 2010. doi:10.1038/nn.2496.
76. **Heitz RP**, **Schall JD.** Neural mechanisms of speed-accuracy tradeoff. *Neuron* 76: 616–628, 2012. doi:10.1016/j.neuron.2012.08.030.
77. **Reppert TR**, **Servant M**, **Heitz RP**, **Schall JD.** Neural mechanisms of speed-accuracy tradeoff of visual search: saccade vigor, the origin of targeting errors, and comparison of the superior colliculus and frontal eye field. *J Neurophysiol* 120: 372–384, 2018. doi:10.1152/jn.00887.2017.
78. **Chafee MV**, **Goldman-Rakic PS.** Inactivation of parietal and prefrontal cortex reveals interdependence of neural activity during memory-guided saccades. *J Neurophysiol* 83: 1550–1566, 2000. doi:10.1152/jn.2000.83.3.1550.
79. **Posner MI**, **Cohen Y.** Components of visual orienting. In: *Attention and Performance*, edited by Bouma H, Bouwhuis D. Hillsdale, NJ: Erlbaum, 1984, p. 531–556.
80. **Cameron EL**, **Tai JC**, **Carrasco M.** Covert attention affects the psychometric function of contrast sensitivity. *Vision Res* 42: 949–967, 2002. doi:10.1016/s0042-6989(02)00039-1.
81. **Yeshurun Y**, **Carrasco M.** Spatial attention improves performance in spatial resolution tasks. *Vision Res* 39: 293–306, 1999. doi:10.1016/S0042-6989(98)00114-X.
82. **Deubel H**, **Schneider WX.** Delayed saccades, but not delayed manual aiming movements, require visual attention shifts. *Ann N Y Acad Sci* 1004: 289–296, 2003. doi:10.1196/annals.1303.026.